Resistive Wall Mode in Collisionless Quasistationary Plasmas

Bo Hu[1] and R. Betti[1,2]

[1]*Laboratory for Laser Energetics and Department of Mechanical Engineering, University of Rochester, Rochester, New York 14623, USA*

[2]*Department of Physics and Astronomy, University of Rochester, Rochester, New York 14627, USA*

(Received 28 January 2004; published 2 September 2004)

The stability analysis of the $n = 1$ resistive wall mode is carried out for a simplified model of collisionless tokamak plasma. It is found that the trapped particle compressibility and the resonance between the mode and the precession drift frequency lead to a significant improvement of the beta stability limits. It is shown that, within the frame of the simplified model, the resistive wall mode can be fully suppressed and the plasma can be stable up to the wall beta limits for a slow plasma rotation.

DOI: 10.1103/PhysRevLett.93.105002 PACS numbers: 52.35.Py, 52.30.–q, 52.55.Fa

The resistive wall mode (RWM) is a macroscopic instability of tokamak plasmas that limits the maximum achievable beta defined as the ratio of the plasma pressure to the magnetic field pressure ($\beta = 2\mu_0 p/B^2$). The RWM is driven by the finite resistivity of the metal vessel (i.e., wall) surrounding the plasma column and by the plasma pressure when the beta exceeds a critical value. Such a critical value (β_∞) corresponds to the beta limits in the absence of the wall and is commonly given in terms of the so-called normalized β defined as $\beta_N = \beta(\%)a[\mathrm{m}]B[\mathrm{T}]/I[\mathrm{MA}]$. According to standard magnetohydrodynamic theory, the RWM is unstable when $\beta_N > \beta_N^\infty \sim 2$–3, and its growth rate is inversely proportional to the resistive wall magnetic diffusion time τ_w. For an ideal superconducting wall, the RWM is stable and the beta limits are set by the ideal external kink that becomes unstable when the normalized beta exceeds a higher critical value (β_N^b) which depends on the wall radius b. However, since the wall resistivity is finite, the RWM prevents the plasma from reaching the higher betas of the wall-stabilized regime. Since the fusion power density increases rapidly with the plasma beta, it is extremely beneficial for a fusion reactor and for future burning plasma tokamak experiments to be able to operate in the wall-stabilized regime $\beta_N^b > \beta_N > \beta_N^\infty$. Several experiments on the DIII-D tokamak and the National Spherical Torus Experiment (NSTX) have indicated that the RWM can be fully suppressed in fast rotating plasmas [1–3]. The fast toroidal rotation is induced by neutral beam injection and its magnitude is a significant fraction of the sound speed. Several authors have theoretically shown that a combination of finite plasma dissipation and fast plasma rotation leads to the suppression of the RWM [4–7]. However, neutral beams in large reactor scale plasmas such as ITER's (International Thermonuclear Experimental Reactor) may not be powerful enough to induce a fast toroidal rotation. For this reason, several researchers are currently developing active feedback stabilization schemes which may mitigate the growth of the RWM in ITER even in the absence of rotational stabilization [8–10]. However, ITER's feedback coils are external to the first wall and vacuum vessel, and are not likely to fully suppress the RWM [10]. Therefore, it would benefit ITER's high-β operation if the wall mode could be stabilized by passive physical effects such as those presented here.

In this Letter, we carry out the stability analysis of the RWM for a simplified model [11] of a large aspect ratio, toroidal, collisionless plasma and show that the RWM may be fully suppressed by the kinetic effects related to the thermal trapped particles in quasistationary plasmas where the rotation frequency is less than the ion diamagnetic drift frequency ($|\Omega_{\mathrm{rot}}| < \omega^i_{*p}$). The trapped particles contribute to the RWM dispersion relation through resonant and nonresonant contributions. The relevant resonant interaction occurs between the RWM and the precession drift frequency of the trapped particle banana orbits. The precession drift frequency of ions or electrons has two components,

$$\omega_D^{i,e} = \omega_E + \omega_B^{i,e},$$

where $\omega_E = -d\Phi/d\Psi$ represents the $\mathbf{E} \times \mathbf{B}$ drift frequency (here Φ is the electrostatic potential and Ψ the poloidal magnetic flux) and ω_B represents the magnetic drift frequency. For a large aspect ratio tokamak, the magnetic drift frequency can be written in the following form:

$$\omega_B \approx \bar{\omega}_B \hat{v}^2 H(u), \qquad \bar{\omega}_B = \frac{q v_{\mathrm{th}}^2}{\Omega_c R r}, \tag{1}$$

$$H(u) = (2s+1)\frac{E(u)}{K(u)} + 2s(u-1) - \frac{1}{2}, \tag{2}$$

where q is the safety factor, v_{th} the thermal speed, $\hat{v} = v/v_{\mathrm{th}}$, Ω_c the cyclotron frequency, R the plasma major radius, r the poloidal radial location, s the magnetic shear, and K and E the complete elliptic integrals of the first and the second kinds. The variable u is defined through $u = 1 + (R/r)(1 - \Lambda)$ with $\Lambda = \mu B/\varepsilon$ being the pitch angle. Finite beta corrections to ω_B are neglected because they are typically small in a large aspect ratio torus with a circular cross section. Those corrections may become

important in realistic high-β tokamak geometry; however, they do not alter the qualitative conclusions of this Letter. Since the RWM is a very low frequency mode with a growth rate of the order of the inverse magnetic diffusion wall time ($\omega \sim \tau_w^{-1} \ll \{\omega_B, \omega_E\}$), a resonant interaction between the mode and the precession drift frequency occurs when $\omega_D - \omega \approx \omega_D \approx 0$. Depending on the direction of the electric field (i.e., the sign of ω_E), the resonance can occur with the ions if $\omega_E < 0$ or with the electrons if $\omega_E > 0$. Neglecting the RWM frequency with respect to ω_B seems appropriate for an ITER-like plasma with a major radius $R \simeq 6$ m, minor radius $a \simeq 2$ m, toroidal field $B \simeq 5$ T, average electron or ion temperature $\bar{T}_{i,e} \simeq 10$ keV, and density $N \simeq 10^{20}$ m^{-3}. The plasma is surrounded by a close-fitting resistive wall with wall time $\tau_w \simeq 0.2$ s [10]. The magnitude of the RWM growth rate varies with β from a few $\tau_w^{-1} \sim 10$ s^{-1} to tens of $\tau_w^{-1} \sim 10^2$ s^{-1} near the ideal wall beta limits before the RWM turns into the ideal kink. Since $\bar{\omega}_B \sim 10^3$ s^{-1} for an ITER-like plasma, then it is appropriate to neglect $\omega \ll \omega_B$ as long as beta is not too close to the wall limits. A critical assumption used here is the one of collisionless plasma species requiring $\omega_B^{i,e} > \nu_{\rm eff}^{i,e}$ where $\nu_{\rm eff} \sim \nu/\epsilon$. For ITER-like parameters, such a condition is satisfied for ion temperatures above $\sim$5 keV and electron temperatures above $\sim$35 keV. Thus, while the ions can be considered as collisionless, the electrons remain collisional even in the hot core of a fusion reactor. Therefore, in order to apply the collisionless theory to ITER, one needs to retain only the ion terms and neglect all kinetic electron terms.

In order to develop a qualitative understanding of the RWM dispersion relation, we include the trapped particle contribution through the kinetic component of the energy principle (the well known δW_K)

$$\delta W_K = \frac{1}{2} \sum_{j=i,e} \int d\mathbf{r} (\tilde{\boldsymbol{\xi}}_\perp^* \cdot \boldsymbol{\kappa}) \tilde{p}_j^K, \tag{3}$$

where $\tilde{\boldsymbol{\xi}}$ is the plasma displacement, $\boldsymbol{\kappa}$ the magnetic field curvature, and $\tilde{p}_j^K$ the nonfluid component of the perturbed trapped particle pressure. The poloidal harmonics of $\tilde{p}_j^K = \sum_m \tilde{p}_j^m e^{im\theta}$ can be derived from the standard solution of the drift kinetic equation for $\omega \approx 0$ leading to

$$\tilde{p}_j^{\,m} = \frac{2^{5/2} \epsilon^{1/2}}{5\pi^{3/2}} \int_0^\infty d\hat{v}^5 e^{-\hat{v}^2} \int_0^1 du K(u) \Pi_j \sigma_m \sum_{\ell=-\infty}^{+\infty} \sigma_\ell \Upsilon_\ell^j, \tag{4}$$

$$\Pi_j = p_j \frac{\omega_E + \omega_{*N}^j + (\hat{v}^2 - 3/2)\omega_{*T}^j}{\omega_E + \omega_B^j}, \tag{5}$$

$$\sigma_m = \int_0^{\pi/2} d\chi \frac{\cos[2(m-q)\arcsin(\sqrt{u}\sin\chi)]}{K(u)\sqrt{1 - u\sin^2\chi}}, \tag{6}$$

$$\Upsilon_\ell^j = \int_{-\pi}^{\pi} \frac{d\theta}{2\pi} e^{-i\ell\theta} \left(\hat{v}^2 \tilde{\boldsymbol{\xi}}_\perp \cdot \boldsymbol{\kappa} + \frac{Z_j e}{T_j} \tilde{\mathcal{Z}} \right), \tag{7}$$

where $\tilde{\mathcal{Z}} \equiv \tilde{\Phi} + \tilde{\boldsymbol{\xi}}_\perp \cdot \nabla\Phi$ represents the electrostatic corrections, which can be obtained from the quasineutrality condition. It is important to retain the electrostatic terms since they enhance the kinetic effects.

The mode-particle resonance induces an imaginary component of the δW_K which fundamentally changes the stability characteristics of the RWM. The RWM dispersion relation in terms of δW's [12] can be rewritten to include the kinetic effects,

$$\gamma\tau_w \simeq -\frac{\delta W_\infty + \delta W_K}{\delta W_b + \delta W_K}, \tag{8}$$

where $\delta W_\infty < 0$ is the fluid energy without wall while $\delta W_b > 0$ is the fluid energy in the presence of an ideal wall with radius b. The opposite signs of $\delta W_{\infty/b}$ indicate that the plasma is in the regime of wall-stabilized ideal kinks and unstable RWM. By separating the resonant (imaginary) and nonresonant (real) contribution to δW_K, it is straightforward to determine the following instability condition for the RWM,

$$(-\delta W_\infty)\delta W_b > |\delta W_K|^2 + \delta W_K^R(\delta W_b + \delta W_\infty). \tag{9}$$

It is important to notice that the δW_K^I term is always stabilizing while δW_K^R can be either stabilizing or destabilizing. For a slow rotation ($|\Omega_{\rm rot}| < \omega_{*p}^i$) and low mode frequency, the dissipation induced by the mode-particle interaction (δW_K^I) is much larger than the typical continuum damping by sound or Alfvén waves. Near the standard no-wall limits where $\delta W_\infty \simeq 0$, the real part is stabilizing if $\delta W_K^R > 0$, while the opposite occurs near the wall limits where $\delta W_b \simeq 0$. Since the no-wall limits are the ones setting the maximum achievable beta in tokamaks, we conclude that a positive δW_K^R is desirable. If $\delta W_K^R < 0$, a stability window opens up near the wall limits but the RWM can become unstable for β's below the no-wall limit and the size of δW_K^I required for full suppression increases. The size of the kinetic terms required for a full suppression of the RWM can be estimated by substituting the heuristic approximations

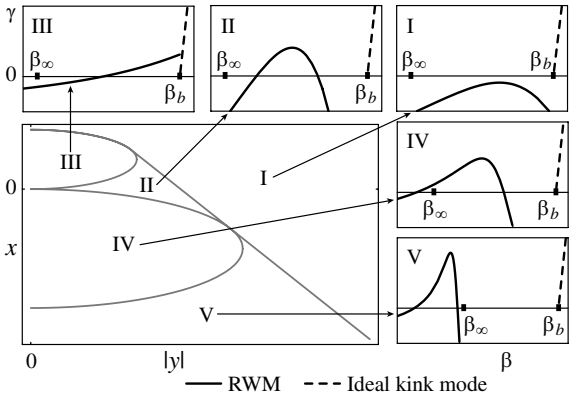

FIG. 1. RWM growth rate behavior (solid lines in small plots) in different regions of the x-y plane (large plot). The dashed curve is the ideal kink growth rate.

$\delta W_\infty \sim (\beta_\infty - \beta)$, $\delta W_b \sim (\beta_b - \beta)$, and $\delta W_K \sim \beta(x + iy)$ into Eq. (9) and extracting the stability conditions for the coefficients x, y representing the size of the nonresonant and resonant particle contributions. A simple calculation shows that the RWM is fully suppressed in region I of Fig. 1 when

$$x(y < y_b) > 0.5[1 - \hat{\beta} + \sqrt{(1 - \hat{\beta})^2 - 4y^2}], \quad (10)$$

$$x(y > y_b) > 1 - 2|y|\sqrt{\hat{\beta}}/(1 - \hat{\beta}), \quad (11)$$

where $\hat{\beta} \equiv \beta_\infty/\beta_b$ and $y_b \equiv (1 - \hat{\beta})\sqrt{\hat{\beta}}/(1 + \hat{\beta})$. Note that Eqs. (10) and (11) indicate that the larger the imaginary part $|y|$, the smaller the real part x has to be in order to achieve the full suppression of the RWM. For a typical case where $\hat{\beta} \simeq 0.5$, the stability condition (10) and (11) requires $x(y < 0.24) > 0.25 + \sqrt{0.06 - y^2}$ and $x(y > 0.24) > 1 - 2.8|y|$. The most severe condition on the size of the real part occurs for $y = 0$ when $x > 0.5$ is required for a full RWM suppression. Figure 1 shows the behavior of the RWM growth rate versus β (small plots) in different regions of the x-y plane (large plot). Full RWM suppression occurs only in region I, while finite stable regions develop in regions II–V. It is worth noting that the instability drive [i.e., the left hand side of Eq. (9)] vanishes at both the wall and the no-wall limits. This constraint on the driving term helps to keep its size numerically small as long as $(\beta_b - \beta_\infty) \lesssim \beta_\infty$. It is therefore appropriate to order the instability drive $-\delta W_\infty \delta W_b \sim \epsilon \delta W_F^2$ where δW_F is the plasma fluid energy and $\epsilon < 1$ is the inverse aspect ratio. Using Eq. (3), it is easy to show that the nonresonant kinetic term δW_K^R scales either as $\sqrt{\epsilon}\delta W_F$ or $\epsilon^{3/2}\delta W_F$ depending on the size of the equilibrium electric field, and therefore its contribution to Eq. (9) is of the same order of the driving term. There is no simple ordering for δW_K^I because of the exponential function in Eq. (4). However, a simple analysis for realistic values of ω_E indicates that $\max[\delta W_K^I] \sim \max[\delta W_K^R]$, thus implying that all the terms in Eq. (9) can be of the same order and the stability of the RWM can be significantly affected by the kinetic effects.

For a quantitative analysis of the trapped particle effects, one needs to solve the full eigenvalue problem. The simple model of a toroidal plasma described in Ref. [11] with a flat pressure and current profiles has successfully been used to solve the eigenvalue problem for the RWM. We follow this approach and find that the kinetic contribution can be easily included after a careful analysis of the terms in the kinetic pressure (4)–(7). It is important to notice that in realistic finite-aspect-ratio diffused tokamak equilibria, all the frequencies in Eq. (5) can be of similar magnitudes and should all be retained. Their relative sizes are important to determine the sign and magnitude of $\tilde{p}^K$ and δW_K. However, in a sharp boundary model, the three frequencies ω_{*N}, ω_{*T}, and ω_E are δ functions, and the sign of $\tilde{p}^K$ is undefined and cannot be related to the actual value for realistic equilibria. In order to capture the essential physics of realistic equilibria, we rewrite Eq. (5) in the following form:

$$\Pi_j = -N_j \frac{R}{2} \frac{dT_j}{dr} \frac{\hat{v}^2 - \frac{3}{2} + \frac{\ell_{T_j}}{\ell_{N_j}} + 2\frac{\ell_{T_j}}{R} w_E^j}{w_E^j + \hat{v}^2 H(u)}, \quad (12)$$

where $w_E^j = \omega_E/\bar{\omega}_B^j$, $\ell_{T_j} = -T_j/(dT_j/dr)$, and $\ell_{N_j} = -N_j/(dN_j/dr)$. The step-function character of the temperature profile is included only in the term dT/dr on the right hand side, which yields $dT/dr = -T\delta(a - r)$. All the other terms containing ℓ_T and ℓ_N are considered as finite and are evaluated using realistic equilibrium profiles at some average radius. Though heuristic, this approach helps to produce results that are possibly in quantitative agreement with the case of realistic tokamak equilibria. Because of the δ-function character (through Π) of the perturbed kinetic pressure, the RWM stability analysis is identical to the one carried out in Ref. [11] except for the boundary conditions at the plasma-vacuum interface which includes the kinetic effects as indicated below,

$$[|p^F + B^2/2|]_a = -\boldsymbol{\kappa} \cdot \hat{n} \int_{a-}^{a+} dr \tilde{p}^K, \quad (13)$$

where p^F is the fluid pressure as defined in Ref. [11]. It follows that the eigenvalue condition for the RWM can be obtained by matching the plasma to the vacuum plus resistive wall solution at the plasma-vacuum interface $r = a$ yielding the kinetically modified version of Eq. (67) of Ref. [11],

$$(\langle q_{Va}^{-2}\rangle - q_a^{-2})m\tilde{\psi}_m/h_m - h_m a\tilde{\psi}_m'/m + \underbrace{\frac{3}{2}\frac{\beta}{\epsilon}\left(\frac{m+1}{h_{m+1}}\tilde{\psi}_{m+1} + \frac{m-1}{h_{m-1}}\tilde{\psi}_{m-1}\right)}_{\text{Fluid instability drive}} + \text{K.T.} = \sum_k \delta_{mk}(\gamma\tau_w)\tilde{\psi}_k, \quad (14)$$

where K.T. is the kinetic term, q_a is the plasma side edge safety factor, $h_m = 1 - m/q_a$, $\tilde{\psi}_m = rh_m B\tilde{\xi}_m(a)/m$, and q_{Va} is the safety factor from the vacuum side. The resistive wall contribution enters through the term δ_{mk} defined in Ref. [11]. The kinetic term in Eq. (14) is obtained by substituting Eq. (4) into Eq. (13), yielding

$$\text{K.T.} = -\frac{1}{2\sqrt{2}\pi}\frac{\beta}{\sqrt{\epsilon_a}}\sum_k\left[\mathcal{K}_{mk}^- r\partial_r + k\mathcal{K}_{mk}^+ + \sum_{l,p}\Delta_{ml}(\mathcal{A}^{-1})_{lp}(\mathcal{B}_{pk}^- r\partial_r + k\mathcal{B}_{pk}^+)\right]\frac{\tilde{\psi}_k}{h_k},$$

$$\mathcal{B}^{\pm}_{pk} = \sum_j Z_j \frac{r}{\ell_{T_j}} \int_0^1 du U_2^j \sigma_p \sigma_k^{\pm},$$

$$\mathcal{A}_{lp} = \sum_j \frac{T_{\rm tot}}{T_j}\left(\frac{\pi\sqrt{\epsilon_r}}{2\sqrt{2}}\hat{\delta}_{lp} - \frac{r}{\ell_{T_j}}\int_0^1 du U_1^j \sigma_l \sigma_p\right),$$

$$\Delta_{ml} = \sum_j Z_j \hat{\theta}_j \int_0^1 du U_2^j \sigma_m^+ \sigma_l,$$

$$\mathcal{K}^{\pm}_{ml} = \sum_j \frac{T_j}{T_{\rm tot}}\hat{\theta}_j \int_0^1 du U_3^j \sigma_m^+ \sigma_l^{\pm},$$

$$U_k^j = \frac{K(u)}{H(u)}\left[V_{k+1}(w_E^j) + \left(\frac{\ell_{T_j}}{\ell_{N_j}} - \frac{3}{2} + 2\frac{\ell_{T_j}}{R}w_E^j\right)V_k(w_E^j)\right],$$

$$V_k(w) = \frac{1}{2\sqrt{\pi}}\int_0^\infty dz \frac{e^{-z}z^{k-1/2}}{z + w/H(u)},$$

where $\sigma_m^{\pm} = \sigma_{m-1} \pm \sigma_{m+1}$, $T_{\rm tot} = \sum_j T_j$, $\hat{\theta}_j = 1/(1 + \ell_{T_j}/\ell_{N_j})$, $\epsilon_r = r/R$, and $\hat{\delta}_{lp}$ is the Kronecker delta symbol. The RWM growth rate is determined by setting to zero the determinant of Eq. (14). We use parameters relevant to the ITER advanced-tokamak scenario [10] characterized by a rather flat q profile with $q \sim 2$–2.5 over 70% of the plasma column, a sharp rise to $q \sim 7$ at the plasma-vacuum interface, and a separatrix ($q \to \infty$) on the vacuum side. In our simple tokamak model, the ITER-like q profile varies from $q_0 = 2.1$ in the center to $q_a = 2.5$ from the plasma side at the plasma-vacuum interface and $q \to \infty$ from the vacuum side at the plasma-vacuum interface. Such a q profile yields the no-wall limits of $\beta_N^\infty \simeq 2.5$ in agreement with Ref. [10]. A close-fitting ideal wall (simulating the effects of ITER vacuum vessel and blanket module) at $b \simeq 1.2a$ yields the ideal wall limits of $\beta_N^b \simeq 4.5$ that are close to those of Ref. [9]. The resistive wall time is $\tau_w \simeq 0.2$ s [10] and $\omega_A \tau_w = 2.4 \times 10^5$. The density and temperature profiles are assumed flat and parabolic, respectively. The gradient scale length ℓ_T in the kinetic terms is computed at $\hat{r} = r/a = 0.7$ where the RWM eigenfunction is large and the ions are still collisionless. The edge average aspect ratio is calculated for an elliptic cross section with $\kappa \approx 1.8$ leading to $\epsilon_a = a\sqrt{\kappa}/R_0 \simeq 0.45$. Nine harmonics $m = 1$–9 are retained to capture all the significant sidebands of the fundamental $m = 3$ mode. For a static plasma ($\Omega_{\rm rot} = 0$), the equilibrium electric field is calculated from the ion equilibrium equation in the absence of flow leading to $\omega_E = -\omega_{*p}^i$ and $w_E^i = -\epsilon_r^{-1}\hat{r}^2/(1 - \hat{r}^2)$. Only the ions are retained as a kinetic species and the kinetic term in Eq. (14) is multiplied by a coefficient $\Theta \leq 1$ in order to study the impact on the RWM stability at different Θ's. The fluid result is recovered for $\Theta = 0$ while the kinetic effects are fully included when $\Theta = 1$. Figure 2 shows the RWM growth rates for different values of Θ, and the RWM is fully suppressed by $\geq 70\%$ of the trapped ion contribution.

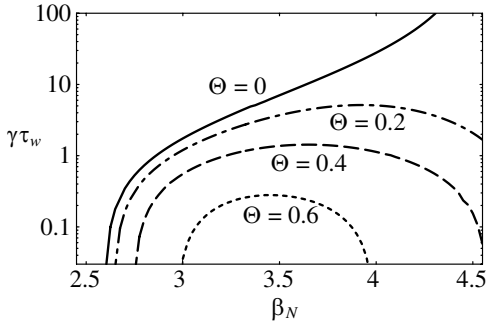

FIG. 2. RWM growth rates versus β_N for different reduction factors $\Theta = 0, 0.2, 0.4, 0.6$.

This important result indicates that the RWM can be suppressed in ITER even in the absence of plasma rotation. The resonance condition and the ion force balance indicate that the stabilizing effect of mode-particle resonance is significant when the plasma rotation is less than ω_{*p}^i and peaks at $\Omega_{\rm rot} \approx \omega_{*p}^i/2$ corresponding to a flow velocity of about 40 km/s for ITER. These stabilizing effects may also play a role in DIII-D and NSTX stability if the high-β regimes are reached in quasistationary plasmas. However, the stabilization may be weaker in smaller tokamaks as the wall time is shorter and the condition $\omega < \omega_B$ is satisfied over a smaller range of β's. Furthermore, fast rotation leads to large electric fields, and large values of $\omega_E \sim \Omega_{\rm rot} \gg \omega_{*p}^i$ hence reduce the kinetic effects of trapped particles. Though the simple model used here includes all the relevant physics, a more accurate assessment of the proposed stabilization mechanism should be carried out for realistic equilibria by modifying existing MHD stability codes.

This work was supported by the U.S. Department of Energy under Contract No. DE-FG02-93ER54215.

[1] E. J. Strait *et al.*, Phys. Rev. Lett. **74**, 2483 (1995).
[2] A. M. Garofalo *et al.*, Phys. Rev. Lett. **82**, 3811 (1999).
[3] S. A. Sabbagh *et al.*, Phys. Plasmas **9**, 2085 (2002).
[4] A. Bondeson and D. J. Ward, Phys. Rev. Lett. **72**, 2709 (1994).
[5] R. Betti and J. P. Freidberg, Phys. Rev. Lett. **74**, 2949 (1995).
[6] J. M. Finn, Phys. Plasmas **2**, 3782 (1995).
[7] R. Fitzpatrick and A. Aydemir, Nucl. Fusion **36**, 11 (1996).
[8] M. S. Chu *et al.*, Nucl. Fusion **43**, 196 (2003).
[9] G. A. Navratil, J. Bialek, A. H. Boozer, and O. Katsuro-Hopkins, Bull. Am. Phys. Soc. **48**, 311 (2003).
[10] Y. Q. Liu, A. Bondeson, Y. Gribov, and A. Polevoi, Nucl. Fusion **44**, 232 (2004).
[11] R. Betti, Phys. Plasmas **5**, 3615 (1998).
[12] S.W. Haney and J. P. Freidberg, Phys. Fluids B **1**, 1637 (1989).